J Intell Robot Syst (2010) 60:181–199
DOI 10.1007/s10846-010-9413-z

Dynamics and Cooperative Object Manipulation Control of Suspended Mobile Manipulators

Mahdy Eslamy · S. Ali A. Moosavian

Received: 5 April 2009 / Accepted: 24 February 2010 / Published online: 11 March 2010

Abstract Dynamics and control of mobile manipulators is obviously a more challenging problem compared to fixed-base robots. Including a suspension system for these mobile platforms increases their maneuverability, but considerably adds to their complexity. In this paper, a suspended wheeled mobile platform with two 6-DOF Puma-type manipulators is used to manipulate an object along a given path. To apply a model-based control algorithm, it is required to have an explicit dynamics model for such highly nonlinear system. This model should be as concise as possible to include fewer mathematical calculations for online computations. Therefore in this paper, a detailed set of dynamics equations for a multiple arm wheeled mobile platform equipped with an effective suspension system is presented. The method is based on the concept of Direct Path Method (DPM), which is extended here for such challenging type of robots. The obtained dynamics model is then verified with a dynamical analysis study using software ADAMS. Then, Natural Orthogonal Complement Method is used to include the non-holonomic constraint of the wheeled platform in a more concise dynamics model. Next, an impedance control law is applied for cooperative manipulation of an object by the two manipulators. The obtained results for a suspended wheeled platform equipped with two 6-DOF Puma-type manipulators reveal a successful performance for moving an object along a mixed circular-straight path, even in the presence of unexpected disturbing forces, system/end-effector flexibility and impacts due to contact with an obstacle.

Keywords Wheeled mobile robots · Suspension system · Dynamics model · Impedance control · Cooperative object manipulation

M. Eslamy (✉) · S. A. A. Moosavian
Advanced Robotics & Automated Systems (ARAS) Laboratory, Department of Mechanical Engineering, K. N. Toosi University of Technology, P.O. Box 19395-1999, Tehran, Iran
e-mail: m.eslamy@gmail.com

1 Introduction

Due to limitations of fixed-base robots, mobile robotic systems have attracted a lot of attentions to perform various tasks in different environmental conditions, [1–3]. Therefore, the trend of academic research has directed towards design, analysis, planning and control of such systems, [4–8], also making plans for employing a group of such systems to perform tasks together, [9, 10]. Unlike fixed-base robots, mobile manipulators can do tasks that may be out of reach of their manipulators by exploiting the mobility of the base platforms. Therefore, the interaction between the base and the manipulators results in more complicated dynamics equations, which in turn requires a more sophisticated control. Obviously, using a suspension system with the mobile platform will add to the complexity of the base-manipulator interactions, however, on the other hand, we will have a system with more flexibility and better performance even in undesirable situations such as moving on uneven environments. Besides, wheeled robotic systems are usually subjected to non-holonomic constraints, [11, 12]. To apply model-based control laws, it is required to extract explicit system dynamics model. To the best of authors' knowledge, not a detailed explicit dynamics model for the suspended mobile manipulators has been suggested in the robotics literature that can be used for model-based control purposes. Saha and Angeles obtained a systematic method for the kinematics and dynamics modelling of a two degree-of-freedom (DOF) Automated Guided Vehicle (AGV), [13]. They have employed the notion of Natural Orthogonal Complement to eliminate the Lagrange multipliers. The dynamic interaction between a 1-Dof manipulator and vehicle of the mobile manipulator is investigated for a planar robotic system, [14]. Direct path method (DPM) has been utilized for deriving the dynamics of a space robotic system equipped with multiple arms which has been proved to have noticeably less time-consuming mathematical calculations as compared to other criteria, [15]. To obtain a concise explicit set of dynamics equations, this useful method is extended in this paper for general terrestrial mobile manipulators equipped with suspension systems, to include the terms induced by considering the gravity and suspension effects on the mobile vehicle.

Various researchers have investigated the methods for motion control of mobile robots. The stable full-state tracking problem for non-holonomic wheeled mobile robots is investigated in [16], where a type (1,1) mobile robot of car-like configuration is studied in detail. Yang et al. have done a research on robust tracking control of constrained wheeled mobile robots with parameter uncertainties and external disturbances by using dissipation theory, where, at end they verified the effectiveness of the proposed control law by simulations, [17]. Yamashita et al. discussed the motion planning of multiple mobile robots during cooperative manipulation and transportation tasks in which they proposed a method for manipulation of large objects in a three dimensional environment, [18]. A scheme to control collective movements of autonomous mobile robots along with a new manipulation method and analyses for obstacle influences was studied in [19].

Object manipulation by robotic manipulators in order to grasp an object and move it according to a defined position and orientation history is an open area of research among the robotics community. An approach for object manipulation using a Barrett Hand and algorithms which involves fuzzy logic and conformal geometric algebra was presented, [20], in which by relating the two mathematical systems they

implement algorithms for geometric computing under uncertainty. Some researcher have investigated the issue of soft object manipulation by the simultaneous control of motion and deformation, [21], they used the symmetric linear mass-damper-spring model to analyze its dynamical behavior then together with feedback control and simulations, the stability of the system was analyzed using the characteristic equation of the coefficient matrix.

A robotic system for fetching objects in home environment is developed in [22], where fetching task is implemented using multimodal user interface (UI) with touch and voice inputs and intelligent adaptive manipulation strategy, based on image processing of images from on-board cameras.

The Multiple Impedance Control (MIC) is a model-based control algorithm that has been shown to have very reasonable results in case of system/object flexibility, contact with an obstacle or disturbance in the system, in comparison with some other approaches and has been developed for several cooperating robotic systems manipulating objects, [23]. The MIC law imposes a reference impedance to all elements of a mobile system, including its base, the manipulator end-points, and the manipulated object itself. This algorithm has been used for space free-flyers and is shown to give good manipulation results even in the presence of impacts due to contact with obstacles, and external disturbances, [24]. Although various control algorithms have been used for control of a mobile platform or for robotic manipulation, manipulating objects by multiple arms mounted on a suspended moving vehicle has remained almost untouched.

The main focus of this paper is on performing object manipulation tasks by multiple manipulators (two Puma 560 manipulators) installed on a wheeled mobile robotic platform equipped with a suspension arrangement. To this end, first using Lagrange method an explicit set of dynamics equations of motion for a general suspended wheeled mobile manipulator are derived in detail based on direct path method (DPM) which is very useful for dynamical and control purposes. These equations are then verified with ADAMS software. Next, the system non-holonomic constraint will be derived, and using Natural Orthogonal Complement Method an independent set of equations of motion for the robotic system is derived. Finally, the MIC law is applied to cooperative manipulation of an object by the two manipulators. Obtained results reveal the merits of the MIC algorithm in terms of negligible small tracking errors even in the presence of impacts due to contact with obstacles, significant disturbances and system/end-effectors flexibility.

2 Dynamics Modeling

2.1 Basic Definitions and Calculations

To express the dynamics of a suspended wheeled robotic system as depicted in Fig. 1, the concept of Direct Path Method (DPM), [15], is exploited. Using Lagrange approach to derive equations of motion for such a system, one can write, [25]:

$$\frac{d}{dt}\left(\frac{\partial T}{\partial \dot{q}_i}\right) - \frac{\partial T}{\partial q_i} + \frac{\partial U}{\partial q_i} + \frac{\partial U_F}{\partial \dot{q}_i} = Q_i \quad i = 1.....N \tag{1}$$

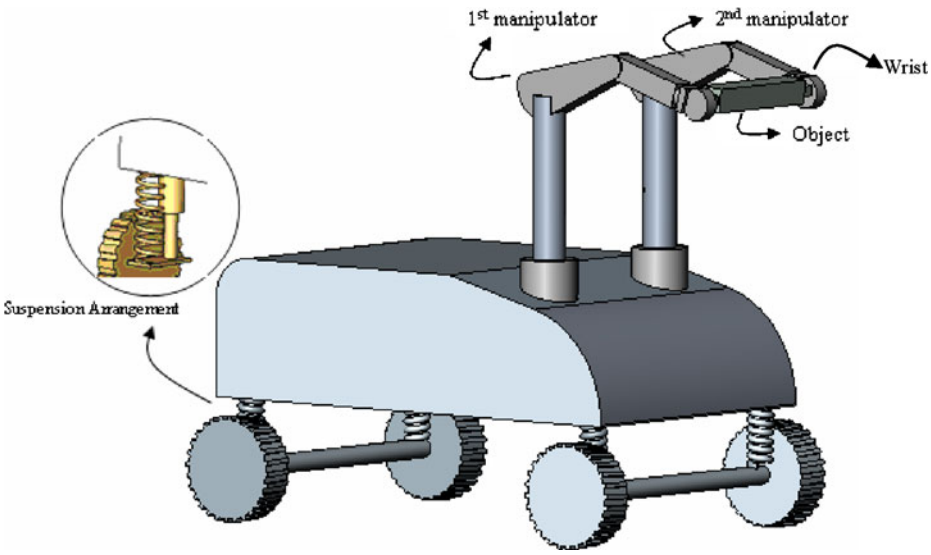

Fig. 1 Suspended wheeled mobile robotic system manipulating an object with two puma560 manipulators

where T, U and U_F are the robotic system's total kinetic, potential and dissipated (due to damping equipments) energy. N describes the system degrees-of-freedom (DOF), q_i, $\dot{q}_i$ and Q_i are the *i-th* element of the vector of the generalized coordinates, speeds, and forces, respectively, as defined below:

$$q = \left\{ R_b^T , \Theta_b^T , \theta_1^T , \theta_2^T , \cdots\cdots , \theta_m^T \right\}^T \tag{2}$$

R_b and Θ_b describe position vector of the vehicle (base) center of mass (CM) and the base Euler angles and $\theta_1, \theta_2, \cdots, \theta_m$ are the vectors of joint angles for the first, second and *m-th* manipulator respectively, as described below:

$$\begin{aligned} R_b &= (x_G, y_G, z_G)^T \\ \Theta_b &= \left(\phi, \theta_r, \theta_p\right)^T \\ \theta_m &= \left(\theta_1^{(m)}, \cdots, \theta_k^{(m)}\right)^T \end{aligned} \tag{3}$$

x_G,y_G,z_G are the vehicle CM positions with respect to the inertial *XYZ* axes coordinates and ϕ,θ_r,θ_p are the base yaw, roll and pitch angles respectively. Finally $\theta_k^{(m)}$ denotes the *k-th* joint variable of the *m-th* manipulator. The puma560 manipulators' Denavit–Hartenberg (D–H) parameters are given in Table 1, [26].

The terms of the total system kinetic energy (T) are explicitly obtained in [15] for a general unconstrained space robotic system. The system total potential energy, U,

Table 1 D–H parameters for puma560

i	$\alpha_{i-1}(^\circ)$	$\theta^{(m)}$
1	0	$\theta_1^{(m)}$
2	−90	$\theta_2^{(m)}$
3	0	$\theta_3^{(m)}$
4	90	$\theta_4^{(m)}$
5	−90	$\theta_5^{(m)}$
6	90	$\theta_6^{(m)}$

contains both gravitational potential energy and the potential energy due to springs tensions or compressions:

$$U = \frac{1}{2}\left(K_1\vec{\delta}_1 . \vec{\delta}_1 + K_2\vec{\delta}_2 . \vec{\delta}_2 + K_3\vec{\delta}_3 . \vec{\delta}_3 + K_4\vec{\delta}_4 . \vec{\delta}_4\right) + m\,\vec{g}\,.\;\vec{R}_b + \sum_{m=1}^{n}\sum_{k=1}^{N_m}\left(m_k^{(m)}\,\vec{g}\,.\;\left(\vec{R}_b + \vec{r}_{c\,k}^{(m)}\right)\right) \tag{4}$$

where g is the gravity acceleration vector, $r_{c\,k}^{(m)}$ and $m_k^{(m)}$ are the position vector of CM for the *k-th* link of the *m-th* manipulator with respect to the base CM and the mass of the *k-th* link of the *m-th* manipulator respectively, $K_1, \cdots, K_4$ are the stiffness coefficient for the springs according to the base four corners, i.e. the front left, rear left, rear right and front right, and $\delta_1, \cdots, \delta_4$ are the corresponding displacements for each spring. Next the system total dissipated energy, U_F, is obtained as:

$$U_F = \frac{1}{2}\left(c_1\dot{\vec{\delta}}_1 . \dot{\vec{\delta}}_1 + c_2\dot{\vec{\delta}}_2 . \dot{\vec{\delta}}_2 + c_3\dot{\vec{\delta}}_3 . \dot{\vec{\delta}}_3 + c_4\dot{\vec{\delta}}_4 . \dot{\vec{\delta}}_4\right) \tag{5}$$

where $c_1, \cdots, c_4$ and $\dot{\vec{\delta}}_1, \cdots, \dot{\vec{\delta}}_4$ are damping coefficients and time rate of corresponding displacements in each suspension equipment in the corners.

2.2 Dynamics Model

Exploiting Lagrange equations, Eq. 1, and substituting the system kinetic, potential and dissipated energies, the dynamics model is obtained as:

$$H(q)\,\ddot{q} + C(q,\dot{q}) + G(q) = Q \tag{6}$$

where the mass matrix (H), non-linear velocity vector (C) and gravity vector (G), are obtained in the following form:

$$H_{ij} = M\frac{\partial\vec{R}_b}{\partial q_i}\cdot\frac{\partial\vec{R}_b}{\partial q_j} + \frac{\partial\vec{\omega}_b}{\partial\dot{q}_i}.I_b.\frac{\partial\vec{\omega}_b}{\partial\dot{q}_j} + \sum_{m=1}^{n}\sum_{k=1}^{N_m}\left(m_k^{(m)}\frac{\partial\vec{r}_{c\,k}^{(m)}}{\partial q_i}\cdot\frac{\partial\vec{r}_{c\,k}^{(m)}}{\partial q_j} + \frac{\partial\vec{\omega}_k^{(m)}}{\partial\dot{q}_i}.I_k^{(m)}.\frac{\partial\vec{\omega}_k^{(m)}}{\partial\dot{q}_j}\right) + \left(\sum_{m=1}^{n}\sum_{k=1}^{N_m}m_k^{(m)}\frac{\partial\vec{r}_{c\,k}^{(m)}}{\partial q_i}\right)\cdot\frac{\partial\vec{R}_b}{\partial q_j} + \left(\sum_{m=1}^{n}\sum_{k=1}^{N_m}m_k^{(m)}\frac{\partial\vec{r}_{c\,k}^{(m)}}{\partial q_j}\right)\cdot\frac{\partial\vec{R}_b}{\partial q_i} \tag{7}$$

Where n is the total number of manipulators mounted on base and N_m denotes the number of the joints of the *m-th* manipulator. Vector C can be written as:

$$C = C_1\dot{\mathbf{q}} + C_2 \tag{8a}$$

where:

$$C_{1\,ij} = M\frac{\partial \vec{R}_b}{\partial q_i}.\left(\sum_{s=1}^{N}\frac{\partial^2 \vec{R}_b}{\partial q_s \partial q_j}\right) + \frac{\partial \vec{\omega}_b}{\partial \dot{q}_i}.I_b.\frac{\partial \vec{\omega}_b}{\partial q_j} + \vec{\omega}_b.I_b.\frac{\partial^2 \vec{\omega}_b}{\partial \dot{q}_i\,\partial q_j}$$
$$+\frac{\partial \vec{R}_b}{\partial q_i}.\sum_{m=1}^{n}\sum_{k=1}^{N_m}\left(m_k^{(m)}\sum_{s=1}^{N}\frac{\partial^2 \vec{r}_{ck}^{(m)}}{\partial q_s \partial q_j}\dot{q}_s\right) + \left(\sum_{s=1}^{N}\frac{\partial^2 \vec{R}_b^{(m)}}{\partial q_s \partial q_j}\dot{q}_s\right).\sum_{m=1}^{n}\sum_{k=1}^{N_m}\left(m_k^{(m)}\frac{\partial \vec{r}_{ck}^{(m)}}{\partial q_i}\right)$$
$$+\sum_{m=1}^{n}\sum_{k=1}^{N_m}\left(m_k^{(m)}\frac{\partial \vec{r}_{ck}^{(m)}}{\partial q_i}.\left(\sum_{s=1}^{N}\frac{\partial^2 \vec{r}_{ck}^{(m)}}{\partial q_s \partial q_j}\dot{q}_s\right) + \frac{\partial \vec{\omega}_k^{(m)}}{\partial \dot{q}_i}.I_k^{(m)}.\frac{\partial \vec{\omega}_k^{(m)}}{\partial q_j} + \vec{\omega}_k^{(m)}.I_k^{(m)}.\frac{\partial^2 \vec{\omega}_k^{(m)}}{\partial \dot{q}_i \partial q_j}\right)$$
$$+\left(c_1\frac{\partial \vec{\delta}_1}{\partial q_i}.\frac{\partial \vec{\delta}_1}{\partial q_j} + c_2\frac{\partial \vec{\delta}_2}{\partial q_i}.\frac{\partial \vec{\delta}_2}{\partial q_j} + c_3\frac{\partial \vec{\delta}_3}{\partial q_i}.\frac{\partial \vec{\delta}_3}{\partial q_j} + c_4\frac{\partial \vec{\delta}_4}{\partial q_i}.\frac{\partial \vec{\delta}_4}{\partial q_j}\right) \tag{8b}$$

and:

$$C_{2i} = -\left(\vec{\omega}_b.I_b.\frac{\partial \vec{\omega}_b}{\partial q_i} + \sum_{m=1}^{n}\sum_{k=1}^{N_m}\vec{\omega}_k^{(m)}.I_k^{(m)}.\frac{\partial \vec{\omega}_k^{(m)}}{\partial q_i}\right) \tag{8c}$$

where ω_b is the vehicle angular velocity, I_b is its mass moments of inertia matrix, while $\omega_k^{(m)}$ and $I_k^{(m)}$ represent those of each link respectively, $\frac{\partial \vec{\delta}}{\partial q_i}$ denotes the rate of the springs displacements with respect to the *i-th* element of generalized coordinates, and finally M is the total mass of the robotic system. Vector G is also obtained as:

$$G_i = K_1\,\vec{\delta}_1.\frac{\partial \vec{\delta}_1}{\partial q_i} + K_2\,\vec{\delta}_2.\frac{\partial \vec{\delta}_2}{\partial q_i} + K_3\,\vec{\delta}_3.\frac{\partial \vec{\delta}_3}{\partial q_i} + K_4\,\vec{\delta}_4.\frac{\partial \vec{\delta}_4}{\partial q_i}$$
$$+m_b\vec{g}.\frac{\partial \vec{R}_b}{\partial q_i} + \vec{g}.\sum_{m=1}^{n}\sum_{k=1}^{N_m}m_k^{(m)}\left(\frac{\partial \vec{R}_b}{\partial q_i} + \frac{\partial \vec{r}_{ck}^{(m)}}{\partial q_i}\right) \tag{9}$$

It should be noted that to calculate the explicit dynamics model of Eq. 6, all its terms, including mass matrix (H), non-linear velocity vector (C) and gravity vector (G), are symbolically computed via Maple.

2.3 Dynamics Model Verification

To validate the obtained dynamics equations, a dynamical analysis study using software ADAMS is presented here to compare with the developed explicit model. Various validation scenarios (such as suspended planar/spatial model with/without manipulators and different road profiles) have been carried out in which some results are discussed in the following. As shown in Fig. 2, a spatial suspended mobile platform with two 3-dof manipulators was one of our validation scenarios (the attached manipulators have the configuration of Puma 560 as shown in Fig. 2 in which each has 3 Dofs (with no wrist)). The surface profile h_i was chosen to be sinusoidal wave in the form of $h_i = a_i \sin\left(2\pi/\lambda_i\,(vt \pm 1)\right)$ for rear/front sides, where v is the vehicle C.M. velocity. The road profile, the suspended vehicle specifications and those of the manipulators which are identical, are given in Tables 2, 3, and 4 respectively. The suspended mobile manipulator modeled in ADAMS is seen in Fig. 2. The obtained results from the verification procedure to compare between

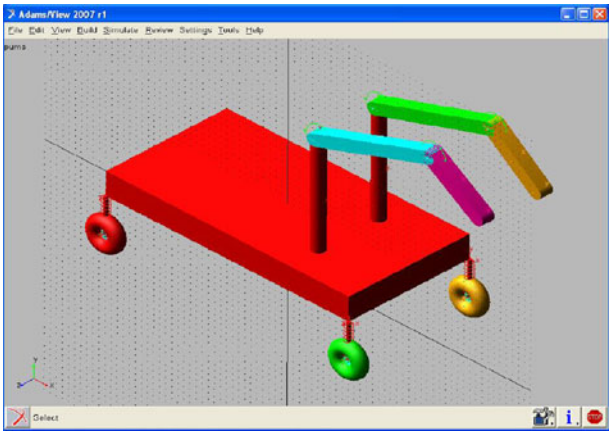

Fig. 2 The suspended mobile manipulator modeled in MSC.ADAMS

ADAMS and proposed explicit model, are depicted in Figs. 3, 4, 5 and 6. The trajectory of each manipulator's joints is defined to be:

$$\theta_1 = 0$$
$$\theta_2 = 1/6\,\pi + 1/600\,\pi\,t^3 - 1/4000\,\pi\,t^4 + 1/100000\,\pi\,t^5$$
$$\theta_3 = 10/9\,\pi + 1/150\,\pi\,t^3 - 1/1000\,\pi\,t^4 + 1/25000\,\pi\,t^5$$

which are the same for both manipulators.

As it is seen, the obtained results from the developed explicit model (programmed in Maple/Matlab), and those of ADAMS software, have a very good agreement with each other. This vigorous study verifies the obtained dynamics model, which now can be employed for simulation studies, and also implementation of model-based control laws.

2.4 Non-holonomic Constraint

Figure 6 illustrates a wheeled mobile robot base that moves by its two rear independent (differentially driver) wheels .The motion of the wheels is restricted to be slipless, therefore the wheels will move along *x′-axis* of rear axle-attached coordinates, Fig. 6. So, one can write, [12]:

$$\vec{V}_{O'} \cdot \vec{j}_{y'} = \circ \tag{10}$$

Table 2 The surface profiles

I	a_i (amplitude (m))	λ_i (wavelength: (m))
1	0.09	0.6
2	0.08	0.6
3	0.12	0.6
4	0.16	0.6

Table 3 Properties of vehicle

Mass (kg)	I (kg/m^2)	Length (m)	Width (m)	Thickness (m)	K (kN/m)	C (kNs/m)	v (m/s)
3,000	[270;1,050;1,300]	2	1	0.2	180	9	2

where $V_{O'}$ is the velocity of the midpoint of the rear axle and $\vec{j}_{y'}$ is the unit vector along y' as shown in Fig. 6. The velocity of the base CM, i.e. point G, can be written as:

$$\vec{V}_G = \vec{V}_O + \vec{\omega}_b \times \vec{l}_{G/O} \tag{11}$$

in which O is the point on base above O' and $l_{G/O}$ is the vector from point O to point G. Using Eqs. 10 and 11 the system non-holonomic constraint will be obtained as:

$$\dot{x}_G \sin(\phi) - \dot{y}_G \cos(\phi) + l\dot{\phi} \cos(\theta_p) = 0 \tag{12}$$

Considering Eq. 12 the DOF of the base at the speed level is reduced to five, as discussed in [12]. The angular velocities of the right and left wheels, i.e. $\dot{\theta}_r$ and $\dot{\theta}_l$, can be chosen as new components of general speeds vector of the base. Then, it can be written:

$$\dot{q} = S(q) \cdot \dot{\nu} \tag{13a}$$

where $S(q)$ is a Jacobian matrix which relates the new general speeds, i.e. $\dot{\nu}$, to the prior ones, i.e. $\dot{q}$. ν is the same as q except for the first three elements in q replaced by left/right rear wheels angles. For the base we have:

$$\begin{Bmatrix} \dot{x}_G \\ \dot{y}_G \\ \dot{\phi} \end{Bmatrix} = Jac_{32} \begin{Bmatrix} \dot{\theta}_l \\ \dot{\theta}_r \end{Bmatrix} \tag{13b}$$

Jac_{32} is a non-square Jacobian matrix which relates the new general speeds of the base to the prior ones as follows:

$$Jac_{32} = \begin{bmatrix} \frac{r}{2}\cos(\phi) + \frac{l_G.r}{b}\sin(\phi)\cos(\theta_p) & \frac{r}{2}\cos(\phi) - \frac{l_G.r}{b}\sin(\phi)\cos(\theta_p) \\ \frac{r}{2}\sin(\phi) - \frac{l_G.r}{b}\cos(\phi)\cos(\theta_p) & \frac{r}{2}\cos(\phi) + \frac{l_G.r}{b}\cos(\phi)\cos(\theta_p) \\ \frac{-r}{b} & \frac{r}{b} \end{bmatrix} \tag{14}$$

In which r is the wheels radius and l_G and b are depicted in Fig. 6. Next, the constraint Eq. 12 can be expressed as:

$$A(q) \cdot \dot{q} = 0 \tag{15}$$

Table 4 Properties of each manipulator links

k-th link	Length (m.)	$M_k^{(m)}$ (kg)	$I_k^{(m)}$ (kg/m^2)
1	1	80	[8;8;0]
2	1	50	[0;5;5]
3	0.5	20	[0;0.5;0.5]

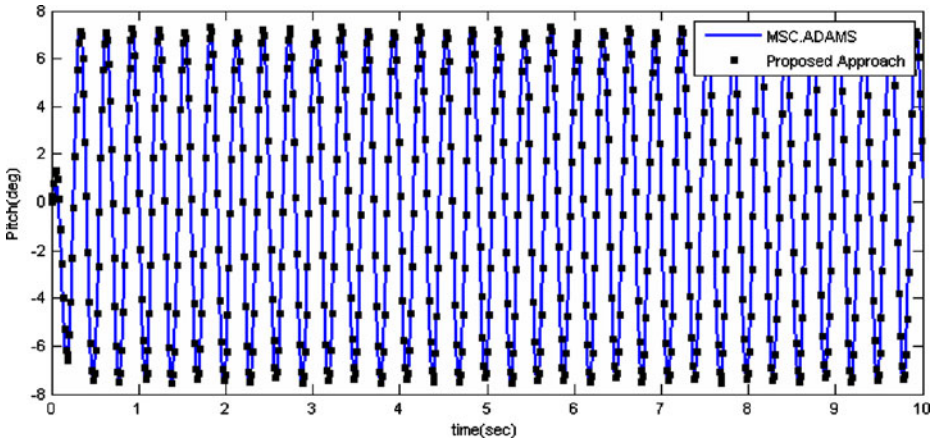

Fig. 3 Variation of the platform pitch angle vs. time; comparison between ADAMS and proposed explicit model

where $A(q)$ is

$$A(q) = \lfloor \sin(\phi) \quad -\cos(\phi) \quad l_G \cos(\theta_p) \quad 0_{1\times(N-3)} \rfloor_{1\times N} \tag{16}$$

Considering (16), and defining corresponding Lagrange multiplier as λ, [13], Eq. 6 can be written as:

$$H(q)\ddot{q} + C(q,\dot{q}) + G(q) + A(q)^T.\lambda = Q \tag{17}$$

Then, using the concept of *Natural Orthogonal Complement Method*, [12], the equations of motion can be derived as a set of unconstrained equations which is

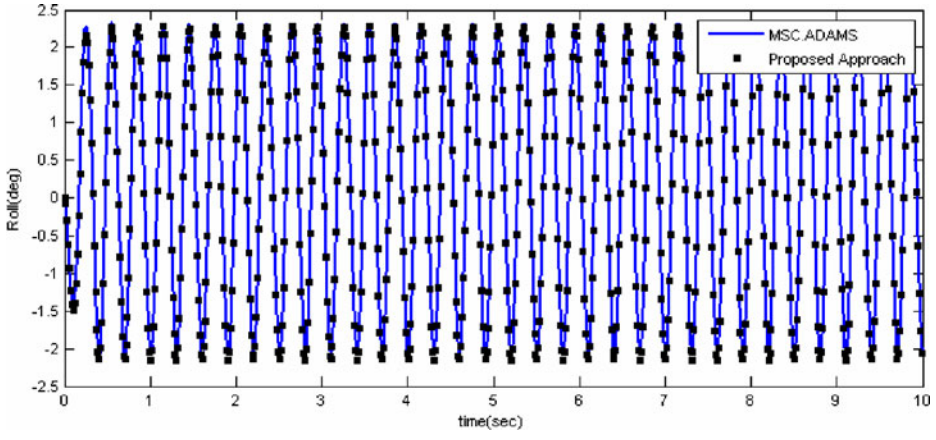

Fig. 4 Variation of the platform roll angle vs. time; comparison between ADAMS and proposed explicit model

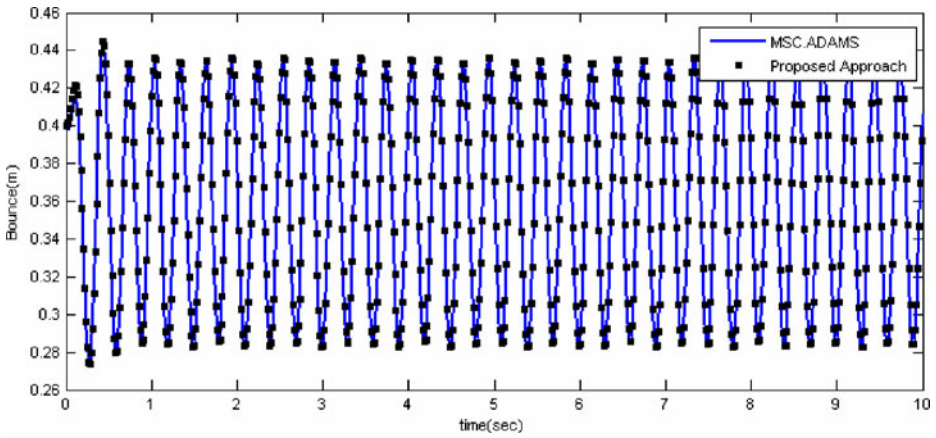

Fig. 5 Variation of the platform vertical pos. vs. time; comparison between ADAMS and proposed explicit model

detailed next. The relationship between constrained general forces and unconstrained ones, can be written as

$$Q_{N\times 1} = E\,(q) \quad \tau_{(N-1)\times 1} \tag{18a}$$

in which $E(q)$ is an $N \times (N-1)$ matrix, and

$$\tau = \left[\tau_l\,,\ \tau_r\,,\ 0\,,\ 0\,,\ 0,\ \tau_1^{(1)},\ \tau_2^{(1)}\,,\ ...,\ \tau_k^{(1)}, ..., \tau_1^{(m)},\ \tau_2^{(m)},\ ...,\ \tau_k^{(m)}\right]^T \tag{18b}$$

Where τ_l and τ_r and $\tau_k^{(m)}$ are the torques to be exerted on the left and right rear driver wheels and the *k-th* joint of the *m-th* manipulator respectively. Based on principle of virtual work, one can write

$$Q^T\,.\,dq\ = \tau^T.\ dv \tag{18c}$$

Substituting dq from Eq. 13a, it is obtained:

$$\tau = S^T\,.Q \tag{18d}$$

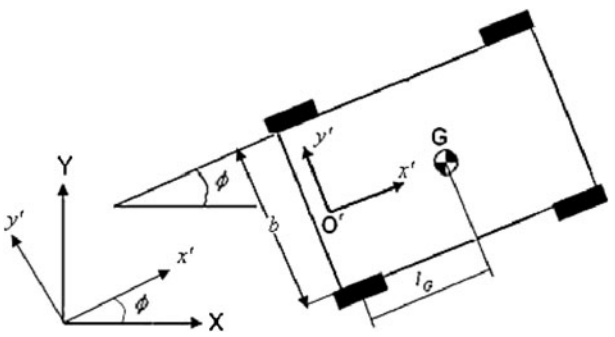

Fig. 6 A wheeled base with no-slippage constraint

Finally, substituting Q from Eq. 18a, we will have

$$S^T \cdot E = 1_{(N-1)\times(N-1)} \tag{19}$$

Now, using (18d) and (19), and multiplying by S^T, Eq. 17 can be rewritten as:

$$S^T \left(H\left(q\right)\ \ddot{q}\ + C_1\,\dot{q} + C_2 + \ G\left(q\right) - E.\tau\right) + S^T\,.\,A\left(q\right)^T\,.\lambda = 0 \tag{20a}$$

Noting the fact that $A(q)$ is in the null space of $S(q)$, the second part will vanish, and (20a) reduces to:

$$S^T H\left(q\right)\ \ddot{q}\ + S^T\,.C_1\,\dot{q} + S^T\,.C_2 + S^T\,.\,G\left(q\right) = \tau \tag{20b}$$

Now, based on Eq. 13a we have:

$$\ddot{q} = S\ddot{v} + \dot{S}\dot{v} \tag{21a}$$

where

$$\dot{S}\left(q,\dot{q}\right) = \begin{bmatrix} \dfrac{\partial Jac_{32}}{\partial t} & 0_{3\times(N-3)} \\ 0_{(N-3)\times 2} & 0_{(N-3)\times(N-3)} \end{bmatrix}_{N\times(N-1)} \tag{21b}$$

Finally, based on (21a) and necessary substitutions in (21b), the equations of motion for the constrained system will reduce into an independent set in the following form:

$$\tilde{H}\,.\,\ddot{v}\ + .\tilde{C}_1.\dot{v} + \tilde{C}_2 + \tilde{G} = \tau \tag{22a}$$

in which

$$\tilde{H} = S^T.H.S \tag{22b}$$

$$\tilde{C}_1 = S^T.\left(C_1 S + H\dot{S}\right) \tag{22c}$$

$$\tilde{C}_2 = S^T.C_2 \tag{22d}$$

$$\tilde{G} = S^T.G \tag{22e}$$

These matrices are symbolically calculated in Maple to obtain concise dynamics model and later are utilized in Simulink together with C-functions for control purposes.

2.5 Jacobian Calculations

The Jacobian matrix for the considered robotic system in case of no constraint will be in the following form

$$\dot{X}_{task} = \ Jac\ \dot{q} \tag{23}$$

where $\dot{X}_{task}$ is the vector of task space speeds that can be in the following form

$$\dot{X}_{task} = \left[\dot{x}_G \quad \dot{y}_G \quad \dot{\phi} \quad \left(\dot{x}_e^1\right)^T \quad \left(\dot{x}_e^2\right)^T\right]^T \tag{24}$$

where x_e^m describes the *m-th* end effector linear position in the inertial frame, and its orientation using Euler angles. Therefore, the Jacobian matrix can be written as:

$$Jac = \begin{bmatrix} 1_{3\times 3} & 0_{3\times(N-3)} \\ Jac^{21}_{(N-3)\times 3} & Jac^{22}_{(N-3)\times(N-3)} \end{bmatrix} \tag{25}$$

As described in (13a), if we use $\dot{\nu}$instead of $\dot{q}$, it is obtained

$$\dot{X}_{task} = \tilde{J}ac\,\dot{\nu} \tag{26}$$

where

$$\tilde{J}ac = Jac \cdot S(q) = \begin{bmatrix} 1_{2\times 2} & 0_{2\times(N-3)} \\ Jac^{21}.Jac_{3\times 2} & Jac^{22} \end{bmatrix} \tag{27}$$

As seen from (27) the new Jacobian matrix is rearranged to reflect the changes of $\dot{q}$ to $\dot{\nu}$. Finally, the time derivative of Jacobian matrix is obtained as

$$\tilde{J}_{dot} = \begin{bmatrix} 0_{2\times 2} & 0_{2\times(N-3)} \\ Jac^{21}_{dot}.Jac_{32} + Jac^{21}.Jac^{32}_{dot} & Jac^{22}_{dot} \end{bmatrix} \tag{28}$$

2.6 Stability Issues

To maintain the mechanical stability, it is inevitable to use a suitable, easy-computed and realistic stability metric that expresses the equilibrium status of the system, [27–30]. Several researchers have tried to propose a suitable criterion for dynamic tip-over stability evaluation. For instance, the Zero Moment Point (ZMP) measure has been utilized for the first time in the context of mobile manipulators by Suagano et al., [31]. It should be noted that in mobile manipulators especially the ones manipulating heavy objects the position of the system center-of-mass (CM) may not be fixed with respect to the base. However, the ZMP, in its original form that was proposed for gait planning in anthropomorphic robots is not sensitive to such variation of CM position, [32, 33]. Another stability criterion has been introduced based on the required energy for placing the CM into a plane (called equilibrium plane) such that the whole moment exerted on the system is minimized, [34]. Although this measure incorporates the inertial forces, but it assumes a fixed direction for the external and inertial forces/torques relative to the base frame during imaginary rotations of the system. The force-angle margin measure, [35], uses the minimum angle between resultant force exerted to the base and tip-over axis normal subjected to the assumption of low velocities. Abo-Shanab and Sepehri have developed a model which takes into account the dynamics of the base that potentially rock back-and-forth in the absence or presence of base compliance, [1]. More recently, a new tip-over stability metric called Moment-Height Stability (MHS) has been proposed for wheeled mobile manipulators, [36]. The proposed metric is physically meaningful based on principal concepts, based on stabilizing and destabilizing moments exerted on the moving base which provides the system mobility, and can be implemented with limited low computational effort. The suggested MHS measure can be effectively used for both legged robots and other mobile manipulators. Application of the MIC law to control multiple-arm wheeled robotic systems while fulfilling the stability requirements based on the MHS measure is an ongoing research.

3 Controller Design

3.1 The Control Law

Multiple Impedance Control (MIC) law is applied here for cooperative manipulation of an object by two manipulators. The MIC law enforces an impedance relationship at the object level, as well as the manipulators-base level, and yields proper results even in the presence of system/object flexibility, disturbant forces and impacts due to contact with the environment. This strategy allows coordinated motion and force control of wheeled mobile robots to perform a desirable manipulation task. A non-model-based version of the MIC law has been recently proposed to be implemented without using system dynamics, and called NMIC, [37]. Therefore, the NMIC law is a quick and more realistic algorithm for implementation in cooperating robotic systems, which can be implemented with reasonable limited on-line computations.

To apply the MIC law, a desired impedance relationship at the object level is written as:

$$M_{des}\ddot{e} + k_d\dot{e} + k_p e + F_c = 0 \tag{29}$$

where M_{des}, k_d, k_p are the desired mass , damping and stiffness matrices, and F_c is the contact force (in contact phase) , and $e = x_{des} - x$ is the object tracking error. On the other hand, as described in [23], the object equation of motion can be obtained as:

$$\mathrm{M}\ \ddot{\mathrm{x}} + \mathrm{F_w} = \mathrm{F_c} + \mathrm{F_o} + \mathrm{G}\ \mathrm{F_e} \tag{30}$$

where M, $\mathrm{F_w}$, $\mathrm{F_o}$, G, and $\mathrm{F_e}$ represent mass matrix, vector of nonlinear velocity terms, external forces/torques, grasp matrix and finally forces/torques exerted by the manipulators end effectors, respectively. As mentioned before, the MIC law enforces the same impedance on various parts of the system. Therefore, we can write the same impedance law for the system as:

$$\tilde{M}_{des}\ddot{\tilde{e}} + \tilde{k}_d\dot{\tilde{e}} + \tilde{k}_p\tilde{e} + F_c = 0 \tag{31}$$

where $\tilde{e} = \tilde{x}_{des} - \tilde{x}$ is the tracking error in the system controlled variables. According to the MIC law the applying forces/torques could be divided in two parts as follows:

$$\tau_{app} = \tau_f + \tau_{mot} \tag{32}$$

where τ_{mot} is the required actuator forces/torques for the motion of the system, and τf is the required forces to be applied on the object by end effectors. The controlling forces/torques τ_{mot} could be calculated based on a feedback linearization approach as follows, [24]:

$$\tau_{mot} = \hat{H}\tilde{M}_{des}^{-1}\left(\tilde{M}_{des}\ddot{\tilde{x}} + \tilde{k}_d\dot{\tilde{e}} + k_p\tilde{e} + \tilde{U}_{fc}F_c\right) + \hat{C} \tag{33a}$$

where

$$\hat{H} = \tilde{J}ac\,\tilde{H}\,\tilde{J}ac^{-1} \tag{33b}$$

$$\hat{C} = \tilde{J}ac^{-1}\tilde{C} - \hat{H}\,\tilde{J}_{dot}\,\dot{v} \tag{33c}$$

$$\tilde{U}_{fc} = \left\lfloor Jac_{31}^T \quad 1_{3\times3} \ldots\ldots 1_{3\times3} \right\rfloor^T \tag{33d}$$

To obtain τ_f, based on the object dynamics, the required controlling force GF_{ereq} could be written:

$$GF_{ereq} = MM_{des}^{-1}\left(M_{des}\ddot{x}_{des} + k_d\dot{e} + k_p e + F_c\right) - F_\omega - F_o \tag{34}$$

The required desired force obtained in (34) could be used to determine τ_f for both manipulators, [24]:

$$\tau_f = \begin{Bmatrix} 0_{2\times 1} \\ GF^1_{ereq} \\ GF^2_{ereq} \end{Bmatrix} \tag{35}$$

It will be shown that by application of the MIC law, all participating manipulators, the moving base and the manipulated object behave with the same desired impedance behavior.

3.2 Disturbance Rejection Characteristics

The effects of the disturbances that are applied on the robotic system are considered here. The resultant generalized disturbance forces/moments can be described as following:

$$Q_{dis} = \sum_{i=1}^{N_b}\sum_{t=1}^{N_f} J_i^{(t)T} Q_{dist,\,t} \tag{36}$$

N_b is the number of the bodies that the disturbant forces are exerted on and N_f is the number of the disturbant forces for the corresponding body, the Jacobian matrix $J_i^{(t)}$ is a $6 \times N$ matrix defined as:

$$\begin{bmatrix} \dot{R}_i^t \\ \omega_i \end{bmatrix} = J_i^{(t)}\,\dot{q} \tag{37}$$

which relates the linear/angular velocities of the *i-th* body to the generalized velocities of the system for the *t-th* disturbant force. Finally the left hand side of Eq. 36 will be added to the right hand side of Eq. 1.

4 Obtained Results and Discussions

The simulated system is shown in Fig. 1, where the moving base is driven with two rear differentially-driver wheels. All geometric and mass properties of the mobile base and each of the two identical manipulators are given in Tables 5, 6. The first manipulator is equipped with remote center compliance (RCC) where its stiffness and damping properties are chosen as, [38]:

$$k_e = 2.4 \times 10^4\,\mathrm{kg/s^2} \text{ and } b_e = 5.5 \times 10^2\,\mathrm{kg/s}$$

and the object parameters are

$$m_{obj} = 10\,\mathrm{kg}, \quad r_e^{(1)} = -r_e^{(2)} = (-0.5, 0, 0)$$

Table 5 Properties of the vehicle platform

Mass (kg)	I (kg/m^2)	l_G (m)	b (m)	r_w (m)	$\tau_{limit}^{left/right}$ N/m
200	[15,40,100]	1.25	1.5	0.25	800

where $r_e^{(m)}$ is the position of the *m-th* end effector with respect to the object center of mass. The springs stiffness and damping coefficients are $K = 3{,}600\,\mathrm{N/m}$, $C = 1{,}100\,\mathrm{Ns/m}$ for the front wheels and $K = 3{,}600\,\mathrm{N/m}$, $C = 1{,}000\,\mathrm{Ns/m}$ for the rear ones. The MIC algorithm is used to successfully move an object in a mixed circular-straight path as depicted in Fig. 7 (right). To examine the capabilities of the MIC law, the object will deliberately face a contact with an obstacle on the straight section of its path at x_w= 5.65 m, where a smooth stop at the obstacle will be desirable. The obstacle is taken as a spring with k_w= 1 *e*5 N/m.

In order to highlight the capabilities of the mobile robotic system together with the MIC law disturbant force equal to $[-650\sin(5t)\ N;\ -650\sin(5t)\ N;\ 350\sin(5t)\ N]$ is applied on the vehicle base on the front right corner during the time t = 2 s to t = 4 s when the robotic system is on its circular path section. The results are depicted in the following figures.

Figure 7 (left) shows the object real path in comparison with the desired one. It is revealed that they have very good correspondence. As it is seen, an accordant motion of both end-effectors results in smooth motion of the object on a 5-m-radius circular path which continues through a straight part at the end of its maneuver, as seen in Fig. 7 (right). The existence of flexibility in the system due to RCC and even the suspension system in the vehicle does not have any permanent undesired effect on the object control which reveals the high capabilities of the MIC law in the presence of flexibility in the system.

Figure 8 (left) shows the change of robot base yaw angle (ϕ) which varies with constant slope on the circular part of its path (until it reaches the straight part), then the base orientation undergoes no change implying that it is going straight forward. Figure 8 (right) shows variation of the contact force, which occurs at the time about t = 13 s. As it is seen its amount is zero during no contact phase, but during contact phase it gradually increases. Based on the MIC law this amounts finally converges to a constant value that is governed by the defined impedance parameters.

Figure 9 (left) shows the left and right wheels torques which shows the wheels react correspondingly, as it is seen because of disturbance, the torques undergo changes but after that, they will converge to their previous amounts. It is seen that the torques also undergo changes which corresponds to the time of switching from the circular part to the straight part of the path at about $t = 6.7$ s which in this case the same disruptions can be seen for the wheels angle error (right) and also at time of contact.

Table 6 Properties of each manipulator links

i-th body	Length (m)	$m_i^{(m)}$ kg	$I_i^{(m)}$ kg/m^2	$\tau_i^{(m)}$ N/m
1	1	10	[1,1,0]	100
2	0.6	7.5	[0,0.2,0.2]	100
3	0.6	5	[0,0.1,0.1]	75
4	0.1	1	[0,0.1,0.1]	75
5	0.1	1	[0,0.1,0.1]	75
6	0.1	1	[0,0.1,0.1]	75

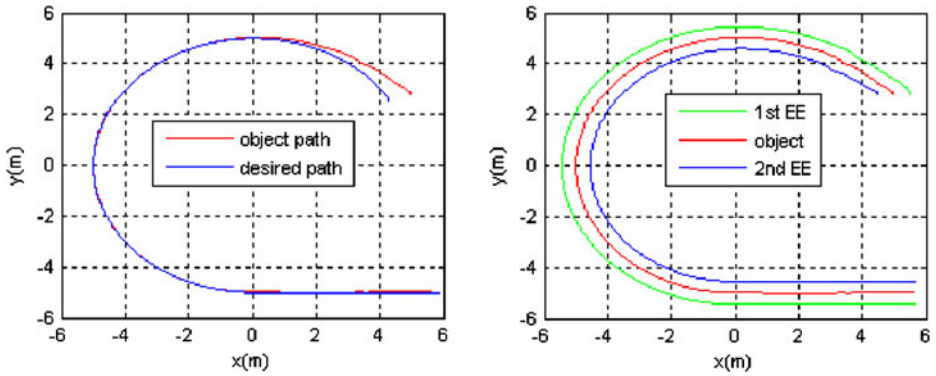

Fig. 7 The object CM real and desired paths (*left*) and object & end-effectors real path (*right*)

Figure 10 (left) shows the variation of the base pitch/roll angles, it is seen exerting disturbance, the angles will experience considerable changes, also during the time of switching from the circular part to the straight part of the path (i.e. $t = 6.7$ s) noticeable changes are seen. The same variations can be seen for the center of mass vertical position for the vehicle base (right).

Figure 11 shows the object , first and second end effectors position error. As it is seen, the disruptions from normal trends correspond to the time of disturbance, switching from the circular part to the straight part of the path, and the impact due to contact with the obstacle. After the contact, the tracking error will undergo a steady error which implies that the MIC law will not allow excessive force to be experienced. In other words, the cause of the steady error lies in the fact that the MIC law concentrates on the dynamical behavior by applying defined impedances both at the object level and the robotic system level, rather than explicit force/position tracking control. So as it is seen the object will come into smooth stop at the obstacle, which shows the success of applying the desired impedance and the merits of the MIC algorithm in terms of smooth performance, i.e. negligible small tracking errors in the

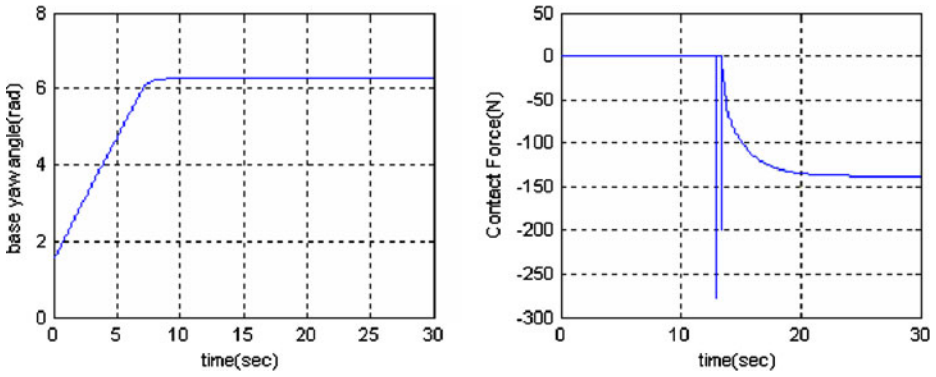

Fig. 8 Variation of the base yaw angle (*left*) and Contact Force (*right*) with time

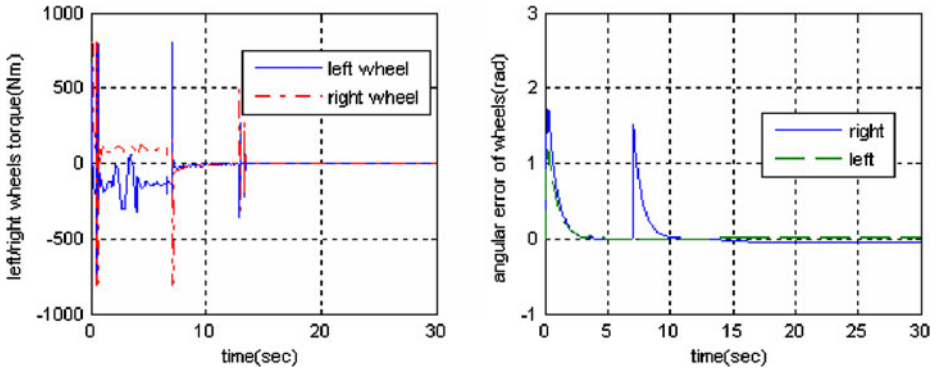

Fig. 9 Variation of the left/right wheel torques (*left*) and angular errors (*right*)

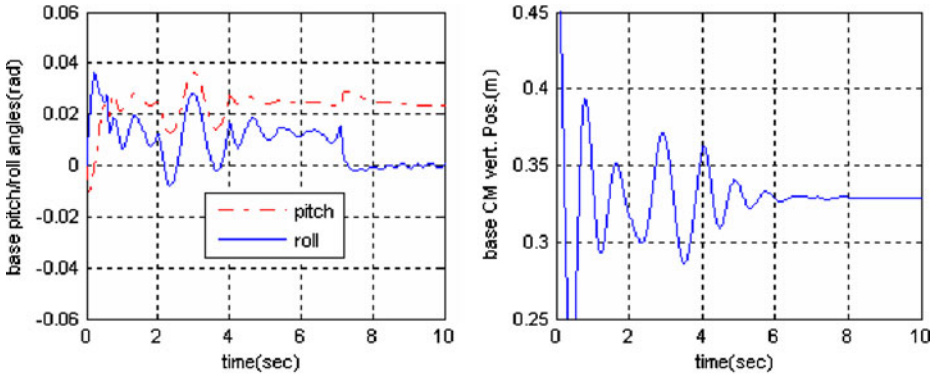

Fig. 10 Variation of the base roll/pitch angle vs time (*left*) and vehicle CM vertical pos. (*right*)

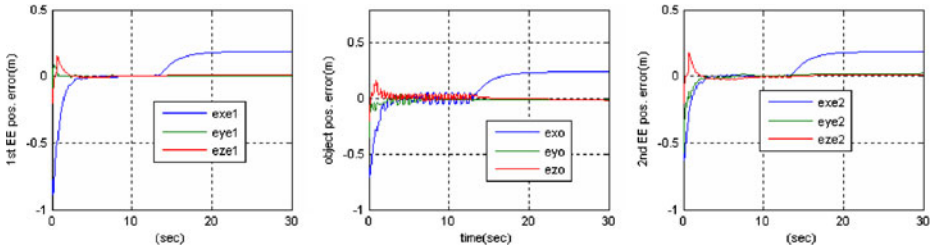

Fig. 11 The 1st end-effector (*left*), object (*middle*) and 2nd (*right*) end effector position tracking error

presence of impacts due to contact with obstacles and significant disturbances and system/end-effectors flexibility.

As depicted, it has to be mentioned that the disturbance has very slight effects on the object and end-effectors tracking errors which shows the robustness of the MIC law.

5 Conclusions

In this paper, using Lagrange method, an explicit dynamics model of a wheeled mobile manipulator with multiple arms and equipped with suspension system, was presented based on the concept of Direct Path Method (DPM), which was extended here for such challenging type of robots. Then the obtained dynamics were verified with ADAMS dynamical analysis software. Next, system non-holonomic constraint was discussed, and using Natural Orthogonal Complement Method an independent set of equations of motion for the suspended robotic system was derived. Finally, the MIC law was applied successfully to manipulate an object by two 6-DOF Puma 560 manipulators, one of them equipped with a remote center compliance (RCC), both mounted on a suspended wheeled platform while the moving base is driven with two rear differentially driven wheels. The obtained results revealed a coordinated smooth motion of the object, manipulators and the moving base, even in the presence of suspension system, impacts due to contact with an obstacle, significant disturbances and system/end-effectors flexibility.

References

1. Moosavian, S., Ali, A., Kalantari, A., Semsarilar, H., Aboosaeedan, E., Mihankhah, E.: ResQuake: a tele-operative rescue robot. ASME J. Mech. Des. **131**(081005), 1–11 (2009)
2. Dalvand, M., Moghadam, M.: Stair climber smart mobile robot (MSRox). Auton. Robots **20**, 3–14 (2006)
3. Huang, H.-C., Tsai, C.-C.: Adaptive robust control of an omnidirectional mobile platform for autonomous service robots in polar coordinates. J. Intell. Robot. Syst. **51**, 439–460 (2008)
4. Alipour, K., Moosavian, S., Ali, A., Bahramzadeh, Y.: Dynamics of wheeled mobile robots with flexible suspension: analytical modeling and verification. Int. J. Robot. Autom. **23**(4), 242–250 (2008)
5. Watanabe, K., Izumi, K., Maki, J., Fujimoto, K.: A fuzzy behavior-based control for mobile robots using adaptive fusion units. J. Intell. Robot. Syst. **42**, 27–49 (2005)
6. Liu, A.-Y., Wu, C.-J.: A discrete method for time-optimal motion planning of a class of mobile robots. J. Intell. Robot. Syst. **32**, 75–92 (2001)
7. Eghtesad, M., Necsulescu, D.S.: Experimental study of the dynamic based feedback linearization of an autonomous wheeled ground vehicle. J. Robot. Auton. Syst. **47**, 47–63 (2004)
8. Klancar, G., Matko, D., Blažic, S.: Wheeled mobile robots control in a linear platoon. J. Intell. Robot. Syst. **54**, 709–731 (2009)
9. Dierks, T., Jagannathan, S.: Asymptotic adaptive neural network tracking control of nonholonomic mobile robot formations. J. Intell. Robot. Syst. **56**, 153–176 (2009)
10. Yu, H., Wang, Y.: Coordinated collective motion of groups of autonomous mobile robots with directed interconnected topology. J. Intell. Robot. Syst. **53**, 87–98 (2008)
11. Yu, Q., Chen, I.-M.: A general approach to the dynamics of nonholonomic mobile manipulator systems. ASME J. Dyn. Syst. Meas. Control **124**, 512–521 (2002)
12. Saha, S.K., Angeles, J.: Dynamics of nonholonomic mechanical systems using a natural orthogonal complement. ASME J. Appl. Mech. **58**, 238–244 (1991)
13. Saha, S.K., Angeles, J.: Kinematics and dynamics of a three-wheeled 2-DOF AGV. In: Proc. of the IEEE Int. Conf. on Robotics and Automation, pp. 1572–1577. Piscataway, USA (1989)

14. Meghdari, M., Durali, M., Naderi, D.: Investigating dynamic interaction between the one D.O.F. manipulator and vehicle of a mobile manipulator. J. Intell. Robot. Syst. **28**, 277–290 (2000)
15. Moosavian, S., Ali, A., Papadopoulos, E.: explicit dynamics of free flyers with multiple manipulator via SPACEMAPLE. J. Adv. Robotic. **18**(2), 223–244 (2004)
16. Wang, D., Xu, G.: Full-state tracking and internal dynamics of non-holonomic wheeled mobile robots. IEEE/ASME Trans. Mechatron. **8**, 203–214 (2003)
17. Yang, T.T., Liu, Z.Y., Chen, H., Pei, R.: The research on robust tracking control of constrained wheeled mobile robots. In: Proc. of the IEEE Int. Conf. on Machine Learning and Cybernetics, pp. 1356–1361 (2005)
18. Yamashita, A., Arai, T., Ota, J., Asama, H.: Motion planning of multiple mobile robots for cooperative manipulation and transportation. IEEE Trans. Robot. Autom. **19**, 223–237 (2003)
19. Kohji, M., Yoshiki, M.: Characteristics of a manipulation system for an autonomous mobile herd. SICE Annual Conference, pp. 2302–2307 (2004)
20. Bayro-Corrochano, E., Machucho-Cadena, R.: Object manipulation using fuzzy logic and geometric algebra. In: Proc. of the IEEE Int. Conf. on Pattern Recognition, pp. 1120–1123 (2006)
21. Shibata, M., Hirai, S.: Soft object manipulation by simultaneous control of motion and deformation. In: Proc. of the IEEE Int. Conf. on Robotics and Automation, pp. 2460–2465 (2006)
22. Taipalus, T., Kosuge, K.: Development of service robot for fetching objects in home environment. In: Int. Sym. on Computational Intelligence in Robotics and Automation, pp. 451–456 (2005)
23. Moosavian, S., Ali, A.: Papadopoulos, E.: Multiple impedance control for object manipulation. In: Proc. of the IEEE/RJS Int. Conf. on Intelligent Robots and Systems, Victoria, B.C, Canada (1998)
24. Moosavian, S., Ali, A., Rastegari, R., Papadopoulos, E.: Multiple impedance control for space free-flying robots. AIAA J. Guid. Control Dyn. **28**(5), 939–947 (2005)
25. Meirovitch, L.: Methods of Analytical Dynamics. McGraw-Hill, New York (1970)
26. Armstrong, B., Khatib, O., Burdick, J.: The explicit dynamic model and inertial parameters of the PUMA 560 arm. In: Proc. of the IEEE Int. Conf. on Robotics and Automation, pp. 510–518 (1986)
27. Dubowsky, S., Vance, E.E.: Planning mobile manipulator motions considering vehicle dynamic stability constraints manipulators. In: Proc. of the IEEE Int. Conf. on Robotics and Automation, pp. 1271–1276 (1989)
28. Huang, Q., Tanie, K., Sugano, S.: Stability compensation of a mobile manipulator by manipulator motion: feasibility and planning. J. Adv. Robotic. **13**(1), 25–40 (1999)
29. Huang, Q., Tanie, K., Sugano, S.: Coordinated motion planning for a mobile manipulator considering stability and task constraints. Int. J. Rob. Res. **19**(8), 732–742 (2000)
30. Abo-Shanab, R.F., Sepehri, N.: Effect of base compliance on the dynamic stability of mobile manipulators. Robotica **20**, 607–613 (2002)
31. Sugano, S., Huang, Q., Kato, I.: Stability criteria in controlling mobile robotic systems. In: Proc. IEEE/RSJ Int. Conf. on Intelligent Robots and Systems, pp. 832–838 (1993)
32. Goswami, A.: Postural stability of biped robots and the Foot Rotation Indicator (FRI) Point. Int. J. Rob. Res. **18**, 523–533 (1999)
33. Vukobratovic, M., Borovac, B.: Zero moment point: thirty five years of its life. Int. J. Human. Robot. **1**, 157–173 (2004)
34. Ghasempoor, A., Sepehri, N.: A measure of stability for mobile manipulators with application to heavy-duty hydraulic machines. ASME J. Dyn. Syst. Meas. Control **120**, 360–370 (1998)
35. Papadopoulos, E., Rey, D.A.: The force-angle measure of tip-over stability margin for mobile manipulators. J. Vehicle Syst. Dyn. **33**, 29–48 (2000)
36. Moosavian, S., Ali, A., Alipour, K.: On the dynamic tip-over stability of wheeled mobile manipulators. Int. J. Robot. Autom. **22**(4), 322–328 (2007)
37. Moosavian, S., Ali, A., Ashtiani, H.R.: Cooperation of robotic manipulators using non-model-based multiple impedance control. J. Indust. Robot. **35**(6), 549–558 (2008)
38. De Fazio, T.L., Seltzer, D.S., Whitney, D.E.: The instrumented remote centre compliance. J. Indust. Robot. **11**(4), 238–242 (1984)